Correlation of Positron Annihilation and Other Dynamic Properties in Small Molecule Glass-Forming Substances

Kia L. Ngai
Naval Research Laboratory, Washington, D.C. 20375-5320

Li-Rong Bao and Albert F. Yee
University of Michigan, Macromolecular Science and Engineering, Ann Arbor, Michigan 48109-2136

Christopher L. Soles
NIST Polymers Division, Gaithersburg, Maryland 20899-8541
(Received 5 June 2001; published 5 November 2001)

Positron annihilation spectroscopy is used to characterize the ortho-positronium lifetime, τ_3, in a broad range of small molecule organic glasses over a wide temperature range. The magnitude and thermal variations of τ_3 reflect changes in the dielectric α-relaxation time τ_α and its non-Arrhenius or "fragile" characteristics. τ_3 also displays striking similarities with the fast relaxations reflected in the hydrogen-weighted mean square atomic displacements $\langle u^2 \rangle$. The parallel temperature variations of $\langle u^2(T/T_g) \rangle$, $\tau_3(T/T_g)$, and $\tau_\alpha(T/T_g)$, and their similar patterns of change between the different glasses, are discussed in terms of anharmonicity in the intermolecular caging potentials and the subnanometer density heterogeneities.

DOI: 10.1103/PhysRevLett.87.215901 PACS numbers: 65.60.+a, 64.70.Pf

Positron annihilation lifetime spectroscopy (PALS) is generally perceived as a structural technique to parametrize the unoccupied volume, or so-called "free volume," of an amorphous polymer. In organic glasses, the ortho-positronium (o-Ps) bound state of a positron has a strong tendency to localize in heterogeneous regions of low electron density. If the heterogeneity is assumed to be a spherical cavity [1,2], the o-Ps lifetime τ_3 can be related to an average cavity or nanopore radius R ($R_0 = R + \Delta R$) where

$$\tau_3 = \frac{1}{2}\left[1 - \frac{R}{R_0} + \frac{1}{2\pi}\sin\left(\frac{2\pi R}{R_0}\right)\right]^{-1}. \qquad (1)$$

Novel studies on zeolites [2–4] support the validity of this approach and find ΔR, the o-Ps penetration depth into the electron cloud surrounding the cavity, to be nearly constant ($\Delta R \approx 1.61$ Å). For organic glasses, it is understood that spherical nanopores are a first order approximation at best. Nevertheless, PALS is widely used to quantify the unoccupied volume in glassy materials.

In the early 1980s, PALS was also used to study dynamics in glass-forming liquids such as ortho-terphenyl (OTP) and various phenyl ethers. Pethrick and co-workers [5–7] correlated thermal variations of τ_3 with the density, free volume, self-diffusion coefficients, and dielectric relaxation behavior [5–7]. However, in the past 20 years there have been limited [8] PALS measurements over an extended temperature range aimed at perceiving the dynamics of small molecule glasses. Meanwhile, considerable experimental and theoretical progress has revealed new trends in both the dynamic and thermodynamic properties for a broad range of glass formers (described in a recent review [9]). In light of these new developments, it is worth revisiting PALS as a tool to probe the dynamics of small molecule organic glass formers. Specifically we present new positron annihilation measurements of three small molecule glass formers, glycerol, propylene glycol (PG), and propylene carbonate (PC), in addition to the previously studied OTP [5–7]. We identify similarities between τ_3 and its temperature variations with several other dynamic properties, including the fast dynamics reflected in the mean-square displacement evidenced by incoherent neutron scattering.

OTP, glycerol, PG, and PC were obtained from Aldrich [10]. The glycerol, PG, and PC were used as received, while the OTP was purified by vacuum sublimation. The PALS spectra were obtained over a wide temperature range, both above and below the calorimetric glass transition temperature. The PALS samples were contained in a disk-shaped cell, approximately 5 mm in diameter and 1 mm thick, sealed on the top and bottom with thin Kapton sheets. The samples were quenched with liquid nitrogen in the chamber of the PALS spectrometer with the data collected on subsequent heating. Phototubes above and below the sample were gated to collect the γ rays coincident with the creation and annihilation of the positrons, thereby determining the lifetime. The conventional PFPOSFIT algorithm [11] was used to deconvolute average o-Ps τ_3 of interest from the spectrum of lifetimes containing much shorter para-positronium (τ_1) and free positron (τ_2) annihilation events.

The thermal variations of τ_3 for the OTP, glycerol, PG, and PC are shown in Fig. 1. In principal, τ_3 corresponds to an average pore radius through Eq. (1). However, over such a small range of τ_3 values, the dependence is *nearly* linear and it is reasonable to assume proportionality

between τ_3 and the nanopore radius. The τ_3 values Fig. 1 correspond to radii $\approx$1.7 to 3.4 Å. However, we present the data in terms of τ_3 so as to not overemphasize the spherical nanopore model. Returning to Fig. 1, the temperatures are scaled by the calorimetric T_g's so that one can compare trends between the different glass formers; T_g's of 158, 167, 190, and 244 K are used for the PC, PG, glycerol, and OTP, respectively.

The thermal variations in τ_3 are qualitatively similar in all of the small molecule glass formers, and consistent with the observations of Pethrick and co-workers [5–7]. At low temperatures there is a relatively weak temperature dependence of τ_3 followed by a crossover to a much stronger dependence at $T/T_g \approx 1$, i.e., the calorimetric glass transition. At sufficiently higher T/T_g, a second crossover is encountered at T_r where τ_3 assumes a slowly varying, almost plateaulike value. This high temperature crossover occurs at $T_r/T_g \approx 1.2$ for OTP and PC and $\approx$1.5 for PG and glycerol.

By now there is a wealth of experimental and theoretical evidence for a distinct crossover between two dynamical regimes in supercooled liquids above their glass transition. These include, but are not limited to, deviations from both the Stokes-Einstein (diffusion and viscosity) and Debye-Einstein (reorientation time and viscosity) relations [12–14], a bifurcation of the α and β relaxation processes [12,15,16], the breaking of ergodicity as predicted by mode coupling theory [17,18], and a crossover between the two Vogel-Fulcher-Tamman (VFT) equations needed to fit relaxation data above T_g [19–24]. Curiously these crossovers occur near $T_r/T_g \approx 1.2$ for relatively "fragile" glass-forming liquids, such as OTP and PC, and at $T_r/T_g \approx 1.5$ for "stronger" glasses like glycerol and PG.

The smaller T_r/T_g window in OTP and PC makes their transitions at T_g and T_r appear very sharp, more so than PG or glycerol. OTP and PC also have relatively large values of τ_3 in comparison to PG and glycerol. Qualitatively this suggests that glasses with relatively inefficient molecular packing and larger unoccupied volume elements (larger τ_3s) display sharper transitions at both $T/T_g \approx 1$ and $T/T_g \approx T_r/T_g$. A sharp transition at T_g implies a greater increase of τ_3 with T/T_g, or enhanced thermal expansion of the nanopores above T_g. Bartos and Kristiak [25] found that a greater "free volume" expansion coefficient corresponds to an increased "fragility" in a series of polymer liquids. This is also consistent with the greater fragility in the OTP and PC.

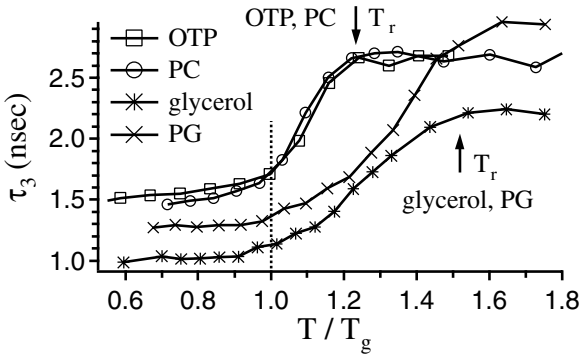

FIG. 1. τ_3 as a function of the T_g-scaled temperature for OTP, PC, PG, and glycerol. A crossover in the thermal dependence of τ_3 is observed both at T_g and an upper temperature T_r, indicated by the vertical arrows. Typical standard uncertainties in τ_3 are $\pm$0.025 ns.

The possible connection between both the magnitude and the sharpness in the thermal transitions of τ_3 with the fragility of the glass former is provocative. As mentioned previously, it now well established [19–24] that the temperature dependence of the structural α-relaxation time, τ_α, or the viscosity of a supercooled liquid must be fit with two separate VFT equations above T_g, with the intersection designated T_B. This relaxation data can be recast in the spirit of the liquid fragility by presenting their steepness indices:

$$m = \frac{\partial \log_{10}(\tau_\alpha)}{\partial(T/T_g)} \tag{2}$$

as a function of T/T_g in Fig. 2 for OTP, PC, glycerol, and PG. The τ_αs in Eq. (2) are taken from Kohlrausch stretched exponential fits, $\exp -(t/\tau_\alpha)^\beta$, to dielectric α-relaxation data reported elsewhere [26,27]. The two VFT fits give rise to two different functions of m with the crossover points, T_B/T_g, indicated by the vertical arrows in Fig. 2.

It is striking that $T_B/T_g \approx 1.2$ for OTP and PC, coincident with the T_r/T_g values in Fig. 1. Likewise, the crossover occurs at $T_B/T_g \approx T_r/T_g \approx 1.5$ in glycerol and PG, implying that $T_B \approx T_r$. The similarities are deeper in that both the τ_3 crossover at T_r and the m crossover at T_B are relatively sharp in OTP and PC; τ_3 and m change rapidly in moving away from the crossover temperature. In contrast, the crossovers are much less dramatic in glycerol and PG; the τ_3 and m variations are gradual in moving away from the crossover temperature. Somehow the unoccupied volume evidenced by PALS reflects the thermal variations of the α-relaxation mechanism. Finally, values of m are much greater near T_g in OTP and PC. This is consistent with their generally greater fragility in comparison to PG and glycerol. Clearly the dynamical characteristics of a supercooled liquid depend upon the level of structural heterogeneity evidenced by PALS. More fragile systems appear to have larger nanopores or heterogeneities as well as pronounced (sharp) thermal transitions. We emphasize that the correlations presented here are based on the *average* τ_3 or nanopore size. It remains to be seen if this is consistent with Novikov and co-workers who state that fragile systems have a more narrow *distribution* of nanopore sizes in comparison to strong glasses [28].

The electron density heterogeneities probed by PALS are typically a few Å in size. For o-Ps to localize, these

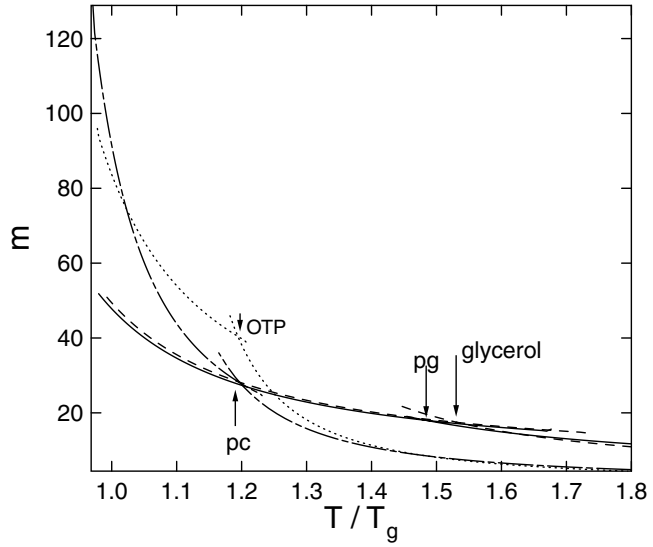

FIG. 2. The steepness index m obtained from fits to the dielectric relaxation data (see text) as function of the T_g-scaled temperature. Two VFT equations are required to fit the data, and the vertical arrows denote the temperature T_B at which the two fits cross over.

defects must persist for at least several nanoseconds. At similar time and length scales, incoherent elastic neutron scattering measures the mean-square atomic displacement, $\langle u^2 \rangle$. $\langle u^2 \rangle$ primarily reflects the intensity of the relatively fast relaxations, the frequency of which depends upon the energy resolution of the spectrometer. For the NG2 High Flux Backscattering Spectrometer [29] at the NIST Center for Neutron Research and the IN10 Backscattering Spectrometer at the Institute Laue-Langevin, the energy resolutions (FWHM) are on the order of 1 μeV. This implies that only motions faster than 0.24 GHz, or time scales shorter than 0.66 ns, give rise to an increase of $\langle u^2 \rangle$; slower motions appear as static. Clearly these time scales are comparable to the minimum o-Ps localization times in a PALS experiment.

The variations of $\langle u^2 \rangle$ ($\approx$1 μeV spectrometers) with T/T_g are shown in Fig. 3. The data for glycerol [30] and OTP [31] are taken from the literature while the PC and PG data are measured on the NG2 High Flux Backscattering Spectrometer. The thermal variations of $\langle u^2 \rangle$ are approximately linear below T_g. If the region $T/T_g < 1$ is fit to a straight line, the inset of Fig. 3 emphasizes the deviations from linearity in the region where $T/T_g > 1$. The thermal dependence of this nonlinear $\langle u^2 \rangle$ bears a striking resemblance to the trends in τ_3 and m observed in Figs. 1 and 2, respectively. Strong increases in the nonlinear $\langle u^2 \rangle$ occur near $T/T_g \approx 1.2$ in OTP and PC and $T/T_g \approx 1.5$ in glycerol and PG. The variations in τ_3, m, and $\langle u^2 \rangle$ are all qualitatively similar across the different glass formers. This is analogous to parallel variations of the fast relaxation process (observed in both neutron and Raman scattering) and the PALS unoccupied volume fraction reported in a few polymeric systems [28,32,33].

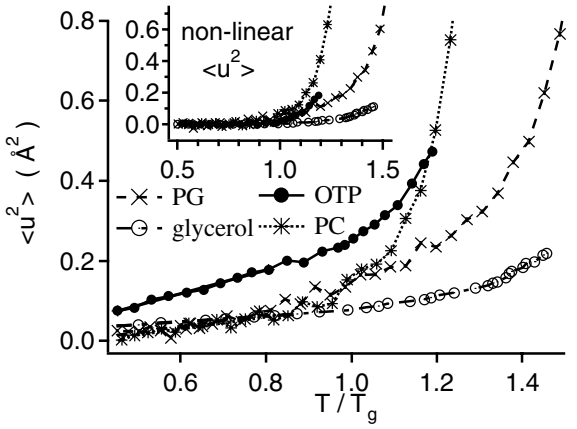

FIG. 3. $\langle u^2 \rangle$ as function of T_g-scaled temperature for OTP, PC, PG, and glycerol. The OTP [31] and glycerol [30] data are taken from the literature. The inset shows the deviations from a linear fit to the data established in the region $T/T_g < 1$. Standard uncertainties in $\langle u^2 \rangle$ are typically less than the size of the data markers.

It is remarkable that the fast relaxations (0.24 GHz or faster) reflected in $\langle u^2 \rangle$ sense the T_g measured from macroscopic variables, like enthalpy or specific volume, at time scales closer to a hundred or a thousand seconds. Even the dielectric relaxation data occurs on a time scale much slower than the neutron scattering $\langle u^2 \rangle$. Stickel and co-workers [24] report that the dielectric α process has a frequency of $\approx 10^{-1}$ Hz at T_g in PC. Granted, these motions can increase very dramatically in frequency over a narrow temperature range. However, even at T_B the dielectric α process is only $\approx 10^6$ Hz in PC [24], still much slower than the $\approx 10^8$ Hz motions reflected in $\langle u^2 \rangle$. For T/T_g less than T_B/T_g, the fast relaxation in $\langle u^2 \rangle$ have little or no direct contribution from the α relaxation

This intriguing behavior can be understood if $\langle u^2 \rangle$ represents the fast relaxation or rattling of an atom or molecule inside the cage of unoccupied volume defined by its nearest neighbors. In a glass this cage is relatively rigid, but heating through the glass transition introduces viscous flow and a sudden increase of the cage size. This would naturally lead to an increase of $\langle u^2 \rangle$. Simulations [34,35] emphasize that while $\langle u^2 \rangle$ is ballistic ($\propto t^2$) at very short times, a time-invariant plateau is observed beyond a picosecond. This plateau indicates caging of the particle and extends for several orders of magnitude in time. Eventually (long times) the particle escapes the cage and a diffusive regime ($\langle u^2 \rangle \propto t$) is entered at the glass transition. A nanosecond resolution places $\langle u^2 \rangle$ well within dynamics of the caged or plateau region. Thus for a strongly caged glass, one expects limited dynamics or a small $\langle u^2 \rangle$.

For a harmonic solid, $\langle u^2 \rangle$ increases linearly with T. The highly nonlinear variations of $\langle u^2 \rangle$ in Fig. 3 thereby indicate anharmonic motions of the caged particles. The picture arises that both τ_3 and $\langle u^2 \rangle$ reflect the level of anharmonicity in the intermolecular or interatomic caging. At very low temperatures, the particles rattle inside these

cages and the o-Ps particles sample the volume available for this rattling motion. Glycerol appears to form a strongly caged glass with harmoniclike motions (linear in $\langle u^2 \rangle$) persisting nearly to T_g. Very strong caging and a low degree of anharmonicity is consistent with the small nanopores (smallest τ_3 values) in glycerol. This is also consistent with the more Arrhenius viscosities or strong characteristics. Conversely, the $\langle u^2 \rangle$ of OTP deviates from linearity well below T_g, indicating an onset of anharmonicity deep in the glassy state. This implies relatively weak caging, supported by the large τ_3 values in OTP, and the relatively fragile characteristics. In short, τ_3 and its temperature dependence provide a measure of the anharmonicity of the caging potential in these small molecule organic glass formers.

K. L. N. is supported by the Office of Naval Research, while L. R. B. and A. F. Y. receive funding from the Air Force Office of Scientific Research, Grant No. F-49620-98-1-0377. C. L. S. is grateful for the assistance from the NIST and the critical discussions with Jack Douglas. The authors further thank the Rob Dimeo and the NIST Center for Neutron Research for access to neutron scattering facilities.

[1] S. J. Tao, J. Chem. Phys. **56**, 5499 (1972).
[2] M. Eldrup, D. Lightbody, and J. N. Sherwood, Chem. Phys. **63**, 51 (1981).
[3] H. Nakanishi and H. Ujihira, J. Chem. Phys. **86**, 4446 (1982).
[4] H. Nakanishi, S. J. Wang, and Y. C. Jean, in *Proceedings of the Conference on Positron Annihilation in Liquids,* edited by S. C. Sharma (World Scientific Publishers, Singapore, 1987), p. 292.
[5] R. A. Pethrick, F. M. Jacobsen, O. E. Morgensen, and M. Eldrup, J. Chem. Soc. Faraday Trans. II **76**, 225 (1980).
[6] B. D. Malhotra and R. A. Pethrick, Phys. Rev. B **28**, 1256 (1983).
[7] B. D. Malhotra and R. A. Pethrick, J. Chem. Soc. Faraday Trans. II **78**, 297 (1982).
[8] J. Bartos and J. Kristiak, J. Phys. Chem. B **104**, 5666 (2000).
[9] K. L. Ngai, J. Non-Cryst. Solids **275**, 7 (2000).
[10] Certain commercial equipment and materials are identified in this paper in order to specify adequately the experimental procedure. In no case does such identification imply recommendation by the National Institute of Standards and Technology nor does it imply that the material or equipment identified is necessarily the best available for this purpose.
[11] W. Puff, Comput. Phys. Commun. **30**, 359 (1983).
[12] E. Rossler, Phys. Rev. Lett. **65**, 1595 (1990).
[13] F. Fujara, B. Geil, H. Sillescu, and G. Fleischer, Z. Phys. B **88**, 195 (1992).
[14] I. Chang, F. Fujara, B. G. G. Heuberger, T. Mangel, and H. Sillescu, J. Non-Cryst. Solids **172-174**, 248 (1994).
[15] C. Hansen, F. Stickel, T. Berger, R. Richert, and E. W. Fischer, J. Chem. Phys. **107**, 1086 (1997).
[16] C. Hansen, F. Stickel, R. Richert, and E. W. Fischer, J. Chem. Phys. **108**, 6408 (1998).
[17] W. Gotze and L. Sjogren, Rep. Prog. Phys. **55**, 241 (1992).
[18] W. Gotze, J. Phys. Condens. Matter **11**, A1 (1999).
[19] K. L. Ngai, J. Magill, and D. Plazek, J. Chem. Phys. **112**, 1887 (2000).
[20] D. J. Plazek and J. H. Magill, J. Chem. Phys. **45**, 3038 (1966).
[21] D. J. Plazek and J. H. Magill, J. Chem. Phys. **49**, 3678 (1968).
[22] R. J. Greet and J. H. Magill, J. Phys. Chem. **71**, 1746 (1967).
[23] F. Stickel, E. W. Fischer, and R. Richert, J. Chem. Phys. **102**, 6251 (1995).
[24] F. Stickel, E. W. Fischer, and R. Richert, J. Chem. Phys. **104**, 2043 (1996).
[25] J. Bartos and J. Kristiak, J. Non-Cryst. Solids **235-237**, 293 (1998).
[26] C. Leon and K. Ngai, J. Phys. Chem. B **103**, 4045 (1999).
[27] K. L. Ngai, J. Chem. Phys. **111**, 3639 (1999).
[28] V. N. Novikov, A. P. Sokolov, B. Strube, N. V. Surovtsev, E. Duval, and A. Mermet, J. Chem. Phys. **107**, 1057 (1997).
[29] P. M. Gehring and D. A. Neumann, Physica (Amsterdam) **241-243B**, 64 (1998).
[30] J. Wuttke, W. Petry, G. Coddens, and F. Fujara, Phys. Rev. E **52**, 4026 (1995).
[31] E. Bartsch, F. Fujara, M. Kiebel, H. Sillescu, B. Farago, and W. Petry, Ber. Bunsen-Ges. Phys. Chem. **93**, 1252 (1989).
[32] A. Mermet, E. Duval, N. Surovtsev, J. F. Jala, A. Dianoux, and A. F. Yee, Europhys. Lett. **38**, 515 (1997).
[33] J. Bartos, P. Bandzuch, O. Sausa, K. Kristiakova, J. Kristiak, T. Kanaya, and W. Jenninger, Macromolecules **30**, 6906 (1997).
[34] C. Donati, S. C. Glotzer, P. H. Poole, W. Kob, and S. J. Plimpton, Phys. Rev. E **60**, 3107 (1999).
[35] P. Allegrini, J. F. Douglas, and S. C. Glotzer, Phys. Rev. E **60**, 5714 (1999).